Electroluminescence Yield in Donor−Acceptor Copolymers and Diblock Polymers: A Comparative Theoretical Study†

Stoyan Karabunarliev* and Eric R. Bittner

Department of Chemistry and Center for Materials Chemistry, University of Houston, Houston, Texas 77204-5003

Received: August 30, 2003; In Final Form: December 10, 2003

The recombination of an electron and hole injected into a nondegenerate π-conjugated polymer is simulated as a relaxation in the excited electronic state space. The rates of the spontaneous one-photon and one-phonon processes are derived within a diabatic model adjusted to the electron−vibrational spectroscopy of PPV. It is shown that the formation of the emissive singlet exciton is accelerated in a regular acceptor−donor copolymer because of the removal of the charge-transfer states. However, the acceptor−donor junction in a diblock heterostructure gives rise to a low-lying polar state that furnishes a nonemissive decay channel. An applied electric field is shown to reduce the luminescence efficiency in the homopolymer and copolymer by polarizing the exciton. In contrast, the quantum yield for the diblock polymer increases with forward bias because of the mixing of the polar exciplex-like state and the exciton.

I. Introduction

Since the discovery[1] of electrically conducting π-conjugated polymers, remarkable progress has been made in their use as active semiconductors in different electronic and optical devices.[2−6] Among those, light-emitting diodes[2] (LEDs) already show device characteristics that are adequate for commercialization. Electroluminescence (EL) involves the radiative recombination of an electron (e) and hole (h) injected into the conduction and valence bands. In a conventional semiconductor, the process is especially efficient at a forward-biased p−n junction where electrons (holes) cross the barrier to reach the hole-rich (electron-rich) region. Charge transport and recombination in a conjugated polymer are more complex because of the nonlinear nature of the electronic excitations in one dimension.[7] Electrons and holes self-localize to form polarons—charge carriers dressed by local lattice distortions. Moreover, the Coulomb interaction is relatively strong, and e−h pairs form bound states (or excitons). Whereas their nature in luminescent polymers such as poly(*p*-phenylenevinylene) (PPV) has been a matter of controversy for some time,[8−11] current estimates put the singlet exciton S_1 around 0.3−0.4 eV below the conductivity threshold of the free e−h pair.[12,13] The triplet exciton T_1 is much more strongly bound and lies about 0.7−0.9 eV lower than the singlet.[14,15] The singlet-to-triplet exciton formation ratio should be 1:3 according to spin-multiplicity statistics. However, there is clear evidence[16−19] that the singlet e−h capture is strongly enhanced when the (effective) conjugation length is large so that the singlet-generation fraction is greater than 50% in highly ordered PPV derivatives.[20−22] The net influence of the electron−phonon (el−ph) interaction on the EL efficiency is ambiguous. On one hand, electron−phonon coupling suppresses charge mobility. On the other hand, it essentially eliminates the self-absorption. The substantial vibronic Stokes shift between absorption and emission in a conjugated polymer renders it similar to a four-level laser system.[3,23]

Along with the development of polymer-based LEDs, the idea of using large molecules as single-electron devices[24] has spurred a quest for molecules with electrical rectification functions.[25] Central to their design has been the model of Aviram and Ratner,[26] who indicated that a donor−acceptor (DA) molecule should behave as an elementary diode. The effect is associated with the existence of a low-barrier charge-separated D^+A^- state, which is generated by injection but decays via intramolecular recombination. The analogy to a semiconductor diode can be readily recognized by identifying the HOMO and LUMO of the donor and acceptor moieties with the valence and conduction band-edges in the p and n regions. Efforts to fabricate such molecules and prove their diode action have resulted recently in the synthesis of a diblock oligomer with thiophene and thiazole as repeat units D and A, respectively.[27] The turn-on voltage of 0.8 eV is commensurate with the offset of their electron affinities and ionization potentials.[28]

Recently, we developed a Coulomb-correlated, electron-vibration model of a single conjugated polymer that relates the Franck−Condon activity in the optical spectra to the interconversion kinetics in excited-state space.[29] The model provides a rationalization of the enhancement of the spin-singlet e−h capture with increasing conjugation length.[19,30] However, in focusing on the spin-dependent branching of the capture process, the concurrent decay kinetics of the excitations to the ground state, S_0, were disregarded. It is well known[2] that apart from singlet−triplet branching the efficiency of EL is largely dictated by the optical coupling of the first excited singlet S_1 with S_0. In the theoretical treatment herein, we include the spontaneous emission rates for the singlet manifold and study the competition between radiative processes, interconversions, and nonradiative decays. This allows us to assess the relative EL yields in a homopolymer, a copolymer, and a diblock system and to model the implications of Stark shifts resulting from the electric field in a device.

† Part of the special issue "Gerald Small Festschrift".

* Corresponding author. E-mail: karabunarliev@uh.edu.

10.1021/jp036587w CCC: $27.50
Published on Web 02/05/2004

SCHEME 1: Localized-Orbital Model of a Two-Band Semiconductor

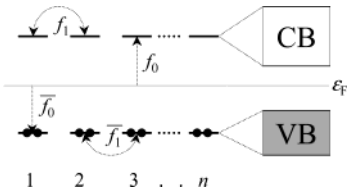

SCHEME 2: Intraunit Monoexcitation and a Charge-Separated e−h Pair

II. Methodology

We consider an array of n two-orbital repeat units that form a two-band 1D semiconductor in the limit of large n (Scheme 1). The relationship with luminescent, nondegenerate ground-state polymers is not apparent because the latter typically have aromatic rings in conjugation and consequently several π valence and π^* conduction bands. Because of this, we have started from the Hartree−Fock (HF) band structure of periodic PPV in the Pariser−Parr−Pople approximation[31] and have explicitly constructed the Wannier functions (WFs) of the highest valence band and lowest conduction band.[29] In the Wannier representation, the interband coupling disappears, the intraunit gap $f_0 + \bar{f}_0$ equals the separation of the band centers, and the first-neighbor transfer integrals f_1 and $\bar{f}_1$ are approximately equal to one-quarter of the bandwidths. The model seems practical for the low-lying excitations in PPV because the frontier bands do not overlap with any other bands and the next-nearest-neighbor transfer integrals are negligibly small. We further adopt a linear electron−phonon coupling that goes beyond the Holstein model[32] in two presumptions. First, the normal modes are nonlocal but form two weakly dispersed optical-phonon branches in the frequency range of the salient Franck−Condon-active modes. Next, the local oscillators modulate not only the energy separation of the monomer Wannier orbitals but also the transfer integrals to their neighbors. Finally, we break the electron−hole symmetry by introducing a slight 5% difference between the one-particle parameters f and $\bar{f}$ for conduction electrons and valence holes.

Excited states are obtained within a simplified monoexcited configuration interaction technique[33] that takes advantage of the fact that the constructed WFs show a small differential overlap.[29] The configuration basis is composed of all possible intraunit monoexcitations and separated electron−hole pairs (Scheme 2). Because the leading e−h interactions show point-charge-like behavior, Coulomb attraction closely follows the Mataga−Nishimoto potential,[34] and spin exchange decays exponentially with separation.

The diagonalization of the CI matrix allows us to transform the model Hamiltonian in its canonical (or diabatic) representation,

$$H = H_{\mathrm{el}} + H_{\mathrm{el-ph}} + H_{\mathrm{ph}} = \sum_a \epsilon_a |a\rangle\langle a| + \sum_{\substack{ab \\ \xi}} g_{ab\xi} Q_\xi |a\rangle\langle b| + \frac{1}{2}\sum_\xi \omega_\xi^2 Q_\xi^2 + P_\xi^2 \quad (1)$$

that includes the vertically excited states (ϵ_a, $|a\rangle$) and the normal modes or phonons (ω_ξ, Q_ξ). Comparison[29] with the experiment includes the separation of the lowest excited singlet and triplet,[14,15] the distribution of the optical coupling over the excited singlet manifold S_a, and the vibronic Stokes shifts and progressions as seen in optical spectroscopy.[35−37] After neglecting singlet−triplet intersystem crossing processes[38,39] as being very slow in the absence of heavy atoms, the model furnishes the basis for studying the dissipative dynamics of electronic excitations.

SCHEME 3: Types of Spontaneous Transitions from a Spin-Singlet Electronic State S_a

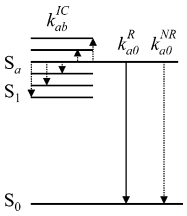

Being coupled to phonons and photons, the multilevel electronic system (1) accommodates two types of spontaneous transitions when not at equilibrium (Scheme 3). As summarized by Kasha,[40] fluorescence occurs essentially from S_1 no matter how the excitation is created. The rule certainly holds for conjugated polymers, keeping in mind that both EL and photoluminescence (PL) originate from the intrachain singlet exciton $S_{XT} = S_1$.[41,42] This implies that internal conversion is the fastest electronic process following the excitation. We identify interconversion kinetics in the excited density of states (DOS) with the nondiagonal form of $H_{\mathrm{el-ph}}$ in eq 1. Assuming that the vibrational bath H_{ph} remains in equilibrium, the rates for electronic transitions with the emission or absorption of a phonon are given by[43]

$$k_{ab}^{\mathrm{IC}} = \pi \sum_\xi \frac{g_{ab\xi}^2}{\hbar\omega_\xi}[1 + \eta(\omega_{ab})] \times [\Gamma(\omega_\xi - \omega_{ab}) - \Gamma(\omega_\xi + \omega_{ab})] \quad (2)$$

Here, η is the Bose−Einstein distribution of the phonons, and Γ is a Lorentzian broadening needed to smooth the discrete phonon spectrum. Note that the one-phonon transitions described in eq 2 are commensurate with the vibrational frequencies and hence occur among the closely spaced S_a excited electronic levels but not across the electronic gap down to the ground state. Whereas the interconversion lifetimes computed in that way fall typically in the 100-ps time scale, the lowest charge-transfer (CT) eigenstates can be much longer lived because of underlying e−h symmetry.[19,29]

The rate for a spontaneous radiative transition $S_a \rightarrow S_0$ is given by

$$k_{a0}^{\mathrm{R}} = \frac{\mu_{a0}^2}{6\epsilon_0\hbar^2}[1 + \eta(\omega_{a0})]\frac{2\hbar\omega_{a0}^3}{\pi c^3} \quad (3)$$

where μ_{a0} is the transition dipole. The latter can be readily estimated from the expansion of the excited-state wave function over localized e−h pairs $|\mathrm{eh}\rangle$,

$$\mu_{a0} = \langle 0|\mu|a\rangle = \sum \mu_{\mathrm{eh}}\langle \mathrm{eh}|a\rangle \quad (4)$$

Here, μ_{eh} represents the transition dipole of the e−h pair, which vanishes with increasing e−h separation. As typical for an intermediate exciton,[44−46] we obtain S_1 to concentrate most of the one-photon coupling with S_0. For an oligomer with $n = 10$ identical R units, the $S_1 \rightarrow S_0$ radiative lifetime

SCHEME 4: Models of a Balanced Charge Injection in a Homopolymer (Top), Copolymer (Middle), and Diblock Polymer (Bottom)

is about 1 ns. This is consistent with what has been observed for PPV-type systems in solution.[42] This shortest radiative lifetime is still much longer than the typical interconversion rates. Hence, it is reasonable to ignore one-photon processes among excited singlets; moreover, they are suppressed by a cubic frequency dependence to a point preventing their detection.

The kinetic model so far presumes that any singlet e−h pair relaxes down the DOS and undergoes radiative decay from its lowest levels. From such a perspective, the photoluminescence yield should approach 1, even if S_1 is only weakly optically coupled to the ground state. To uncover the relationship between EL efficiency and electronic structure, it is necessary to contemplate the nonemissive processes to S_0. This issue remains beyond the scope of the present molecular model, keeping in mind that nonradiative decay channels are typically provided by the intermolecular environment. In rough agreement with the average experiment,[42] we take a nonradiative decay rate $k_{a0}^{NR} = 1\ ns^{-1}$ for each excited state. Under this premise, it is clear that, within the kinetic model, radiative decay to the ground state will prevail if the phonon-mediated relaxation in the DOS populates rapidly emissive eigenstates around its bottom.

III. Results and Discussion

Excited States. By offsetting the localized orbital energy levels of the monomers, our model can be extended from a homopolymer (HP) to a copolymer (CP) and a diblock polymer (DP) (Scheme 4). Whereas the electron affinity and ionization potential are assumed to shift in parallel by 0.8 eV on going from an acceptor (A) to a donor (D) repeat unit, the energy separation of the localized orbitals and the other parameters (e.g., one- and two-body integrals and el−ph coupling strengths) are taken to be the same as for PPV.[29] Scheme 4 also illustrates the hypothetical initial state created by a balanced charge injection into the far ends of the chain. In the heterosystems, we limit our attention to the low-barrier injection with configuration $D^+...A^-$ and consider single chains with $n = 32$ repeat units. Whereas the effective conjugation in highly ordered polymers can extend further than that,[8,11] the finite n is not expected to obscure the HP−CP−DP differences in electronic structure and the ensuing nonequilibrium kinetics.

Figure 1 shows the computed singlet excited-state densities for HP, CP, and DP. The distribution is essentially continuous because $n = 32$ entails more than 1000 excited spin states. The obtained DOS for HP diverges substantially from the joint density of one-particle states in a 1D semiconductor.[8] The Coulomb interaction removes the band-edge singularities inherent in the tight-binding model and gives preference to bound states at the bottom. The exciton $S_{XT} = S_1$ in HP is depicted in Figure 2 by its projection onto the localized e−h pairs. As seen there, S_{XT} is composed mainly of intraunit and short-range e−h pairs. These have the largest dipole matrix element with S_0; therefore, S_{XT} is found to dominate the one-photon spectrum.

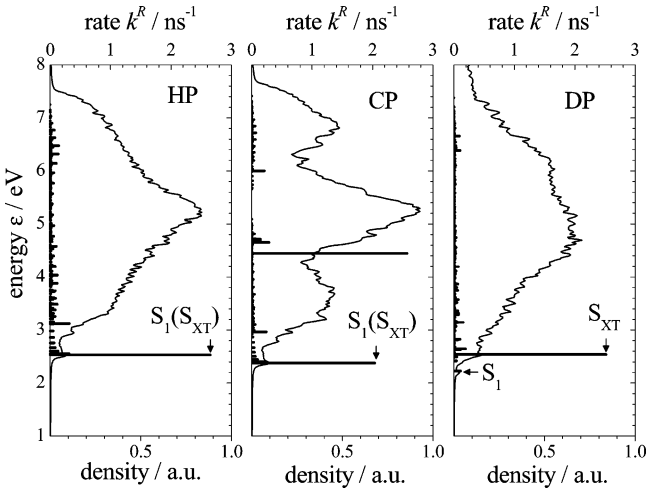

Figure 1. Density of states and emission rates (bars) for the singlet manifold in the model homopolymer (HP), copolymer (CP), and diblock polymer (DP). Energy levels are taken with a line width of 0.03 eV in the density distributions.

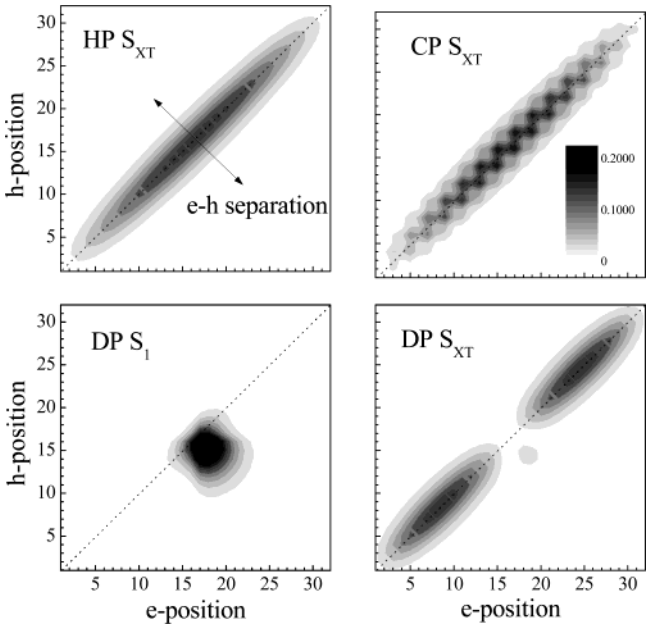

Figure 2. Low-lying excited states as projections onto the localized e−h pairs.

As shown in Figure 1, S_{XT} has the highest spontaneous emission rate. The one-photon transition probabilities of the higher-lying S_a appear to be much smaller because the intraunit e−h pairs in the linear expansions tend to be out of phase. The first excited singlet preserves its exciton character in CP. The expansion of S_{XT} in this case (Figure 2) is consistent with a local polar pattern, where the low-energy D^+A^- configurations prevail completely. This is why its energy is by about 0.15 eV lower than in HP. However, the polar admixture of S_{XT} in CP does not markedly lower its one-photon coupling with S_0 (Figure 1).

The red shift of the exciton in a copolymer could be much more pronounced if the covalent interunit coupling was smaller. The singlet exciton in thin-film polyfluorene is around 3.0 eV,[47] consistent with a weaker interunit conjugation than in PPV. However, the optical gap of the poly(fluorene-*co*-benzothiadiazole) derivative is about 2.4 eV,[47] which is due to both the overall electrophilic offset of the frontier orbitals of benzothiadiazole and their smaller separation.[48]

For the diblock polymer, the exciton at ∼2.5 eV is strongly dipole-coupled to the ground state, with a natural radiative

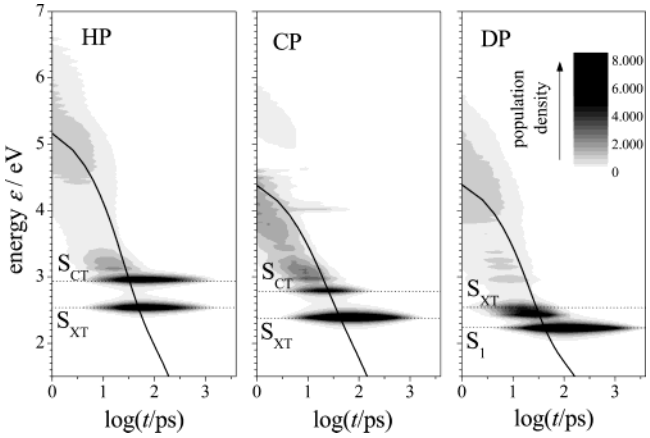

Figure 3. Excited-state population during recombination as a function of energy and time. Model systems are the same as those in Figure 1. The energy of the relaxing superposition electronic wave function is given by the solid curve. Dotted lines mark the essential excited eigenstates.

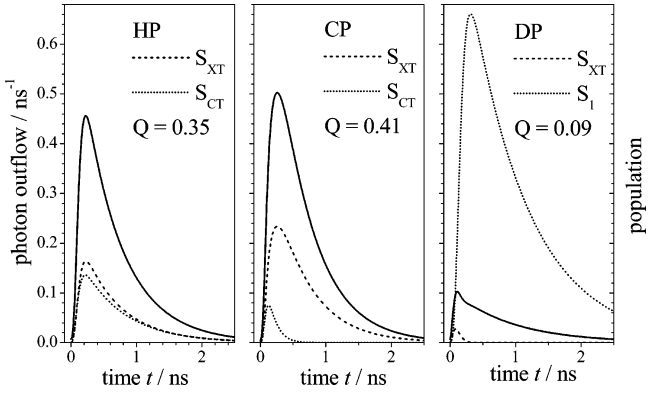

Figure 4. Time-dependent photon outflow (solid curves) and excited-state populations (dashed and dotted curves) in the model systems. Quantum yield (time-integrated outflow) is denoted by *Q*.

lifetime of 0.5 ns. As seen in Figure 2, its wave function is similarly dominated by intraunit e−h pairs but is interrupted at the block boundary. The DA junction not only acts as a conjugation break for the exciton wave function in this case but also gives rise to a polar first excited state about 0.3 eV below the exciton. As illustrated in Figure 2, its wave function is composed of short-range D^+A^- pairs confined to the heterojunction. Notably, the radiative lifetime of this low-lying intramolecular exciplex is foreseen to be very long because of the separation of the electron and hole.

Recombination Kinetics. The simulated process of singlet e−h recombination is illustrated in Figure 3 by the time-dependent population density in the excited-state space. The logarithmic time scale extends to 4 ns after the initial charge injection. The contour plots illustrate the superposition quantum state that simultaneously relaxes down the DOS and decays into S_0 (zero energy level not shown). Its energy as a function of log(*t*) is close to linear, suggesting a near-exponential dissipation. The slight change in the slope of the curves around $t = 10$ ps is concomitant with the onset of radiative decay once the interconversion reaches the low-lying exciton-like states.

For HP, the phonon-mediated relaxation in the excited-state space is seemingly completed in about 100 ps with the formation of the exciton S_{XT} and the lowest charge-transfer state S_{CT}. Whereas S_{XT} coincides with S_1 and is the natural interconversion endpoint, the formation of S_{CT} is due to the approximate electron−hole symmetry of hydrocarbon systems.[19,29] Excited states in such systems are odd or even upon e−h transposition. Whereas S_{XT} is the lowest even-parity state, S_{CT} is the lowest odd-parity state composed exclusively of separated e−h pairs. Even- and odd-parity states are not vibronically coupled under e−h symmetry. The corresponding interconversion rates remain much slower than those between same-parity excited states even when the symmetry is lifted. The initially injected e−h pair corresponds to a mixed-parity wave function, whose even- and odd-parity components relax to S_{XT} and S_{CT} on a 10- to 100-ps time scale via parity-preserving processes. The subsequent symmetry-forbidden conversion of S_{CT} to S_{XT} already falls in the nanosecond range and parallels the decay to S_0. Generally, the cumulative $S_{XT} \rightarrow S_0$ decay rate is much faster than that of $S_{CT} \rightarrow S_0$ because of the dominant radiative component. However, because $S_{CT} \rightarrow S_{XT}$ interconversion is still occurring, S_{XT} remains populated longer than its radiative lifetime. (See also Figure 4.)

Turning to the recombination process in CP, we first note that the injection barier is lowered by 0.8 eV (Figure 3). Also, the DA alternation along the chain destroys the e−h symmetry and smears the distinction between odd- and even-parity wave functions. The time-dependent population density for CP still shows the signature of a long-lived S_{CT} at about 2.8 eV, but its conversion to S_{XT} is much faster than for the homopolymer. A change in the kinetics of the injected e−h pair is also evident from Figure 4, in which the S_{XT} population transient for CP substantially surpasses that of S_{CT}.

Relaxation to the bottom of the DOS appears to be even more rapid in DP. Here, S_1 reaches a peak population of 0.65 as compared to about 0.5 in HP and CP. In Figures 3 and 4, we also see that the S_1 state in DP is longer-lived. The reason for this is that its decay to the ground state is nearly nonemissive and consequently slower.

Figure 4 suggests that the EL efficiency decreases significantly on going from HP and CP to DP. The quantum yield *Q* from singlet e−h pairs is observed to change thereby from about 0.4 to less than 0.1. When comparing photon outflows, exciton populations (Figure 4), and radiative rates (Figure 1), it becomes apparent that luminescence in HP and CP comes exclusively from the exciton. For the DP system, the exciton gives rise to a short initial peak in the emission, but the tail is due to the weak emission from the long-lived S_1 state. In summary, the heterojunction in DP is foreseen to act as a luminescence quencher by giving rise to a near-dark exciplex-like state.

Effect of Drive Voltage. Polymer-based LEDs are usually driven by electric fields of 10^5 to 10^6 V/cm.[2] This corresponds to 0.006 to 0.06 V per monomer when applied parallel to a linear PPV chain. Here, we adopt a ramp potential forward to the charge injection with the typical gradient of 5×10^5 V/cm[49] and assume that this shifts the localized orbitals of neighboring monomers by 0.03 eV relative to each other. The computational methodology remains the same in all other aspects. We omit the illustration of the predicted Stark-shifted density of states and turn directly to the ensuing population kinetics in the energy representation (Figure 5). The essential electronic states are discernible by the transient peaks in the population density. Their zero-field positions are marked by dotted lines. The exciton S_{XT} is practically unperturbed because its substantial Coulomb binding precludes field-driven polarization. The states with symmetry-imposed e−h separation experience, in difference, substantial Stark shifts. The S_{CT} state in HP and CP acquires a dipole moment and shifts down substantially. The exciplex-like S_1 state in DP is polarized oppositely to the drive bias and is raised by about 0.07 eV from its zero-field position. Although relatively small in terms of energy, the Stark shifts of the charge-

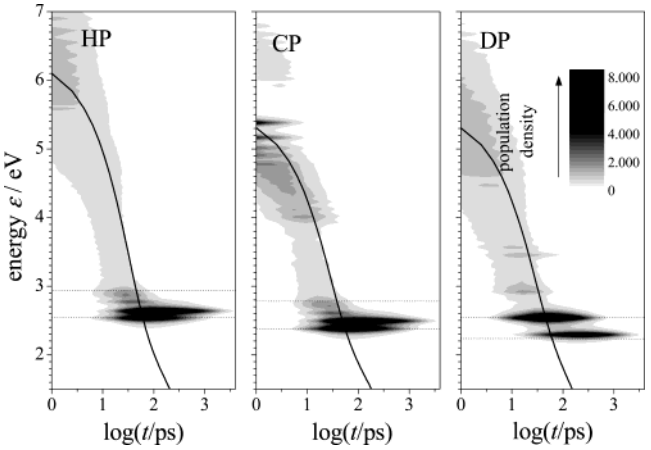

Figure 5. Excited-state population as a function of energy and time in the presence of drive bias. Dotted lines mark the characteristic zero-field excited levels as in Figure 3.

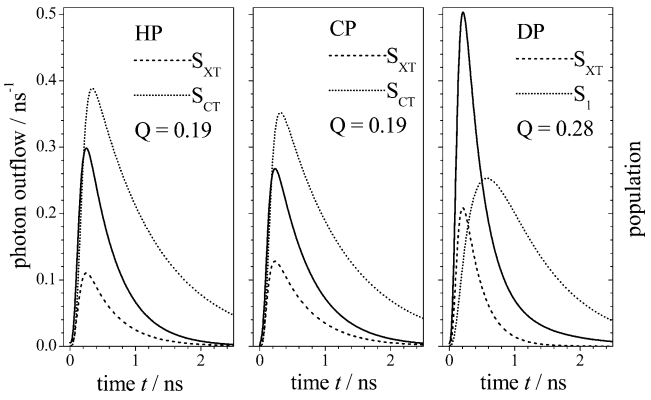

Figure 6. Time-dependent photon outflow (solid curves) and excited-state populations (dashed and dotted curves) in the presence of forward voltage bias.

transfer states affect the recombination kinetics. Comparing Figures 3 and 5, we notice that the charge-transfer state, S_{CT}, is more populous and longer-lived in HP and CP and that the opposite applies to the exciton. In contrast, the formation of S_1 in DP is suppressed, and the fast IC process converges predominantly into the exciton at 2.53 eV. Because, as in the zero-field case, the exciton remains the dominant emissive channel, luminescence is weakened in HP and CP but strengthened in DP (Figure 6). Upon bias, the quantum yield decreases by about 50% in HP and CP but increases by a factor of 2 in DP. The improvement in EL efficiency in DP can be traced to the field-induced mixing of S_{XT} and S_1. Forward bias increases the population transient of S_{XT}. Furthermore, it brings the electron and hole in the S_1 state closer together, improving their probability to recombine. It can be anticipated that EL from DP will be most efficient when S_{XT} and S_1 become degenerate and indistinguishable. In this respect, we note that the assumption of a uniform distribution of the bias over the DP chain is very dubious. In a conventional diode heterostructure, applied voltage essentially lowers or raises the barrier at the interface. One can similarly hypothesize that in the presence of a hole-transporting donor segment and an electron-transporting acceptor segment the resistance of the DP chain will be concentrated at the block boundary. Therefore, it is reasonable to expect that the position of S_1 will be sensitive to the applied voltage rather than the field average and consequently much more tunable.

From a broader perspective, the intramolecular heterojunction addressed herein has intermolecular analogues in polymer blends

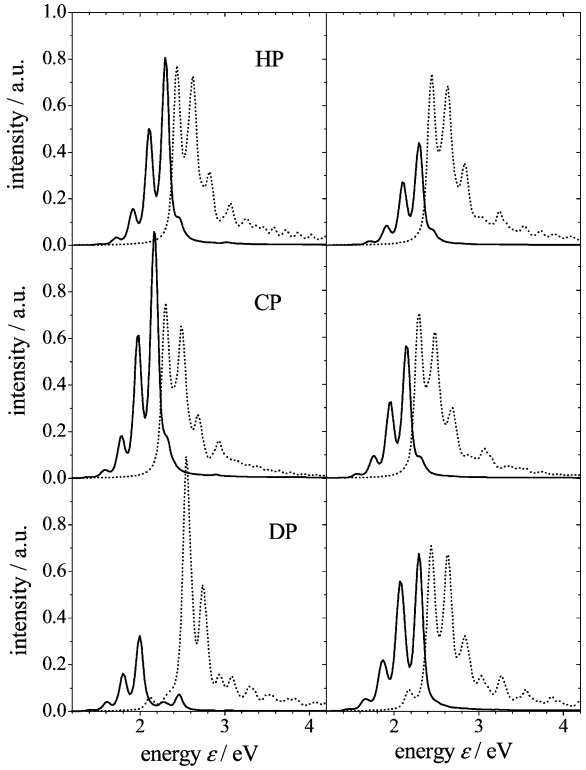

Figure 7. Time-integrated EL spectra and ground-state absorptions of the model system without (left) and with (right) drive bias. Luminescence spectra reflect the difference in quantum yield.

of polyfluorene-based copolymers,[50] whose time-resolved luminescence reflects both the short-lived exciton and the lower-lying exciplex with a much longer radiative lifetime.[51] More recent studies[52] also show that the luminescence yield and dynamics at the polymer heterojunctions are essentially electric-field-dependent in a way that is largely consistent with the present model.

Spectral Band Shapes. Keeping in mind that self-absorption is detrimental to light generation in the material, it is useful to assess the overlap between single-molecule emission and absorption. The time-integrated fluorescence spectra for a single recombination act in HP, CP, and DP are shown in Figure 7, together with the absorption spectra from the ground state. In this case, we turn to the adiabatic representation of the excited states and compute the spectrum in the Condon approximation as a superposition of the electron−vibrational transitions with a relatively small line width (0.03 eV). This ad hoc approach is admittedly in conflict with the diabatic approximation used to compute transition rates and time-dependent populations. However, it affords a better comparison with the low-temperature optical spectra of conjugated polymers and roughly reconstructs the observed vibrational progressions and Stokes shifts.[35−37]

The absorptions of the model systems are very similar. In all cases, the leading contribution comes from the $S_0/0 \rightarrow S_{XT}/\nu$ progression in C═C bond stretches, whose vibrational features are broadened by the low-frequency librations.[53−55] Significant tailing of the absorption ensues also from the higher-lying optically coupled eigenstates. In DP, the absorption of the near-dark S_1 is discernible as a shoulder on the low-energy side of the S_{XT} band. Whereas the electric field is not foreseen to change the absorption for HP and CP substantially, it has a marked impact on the DP spectrum. In the DP case, the strength of the $S_0/0 \rightarrow S_{XT}/\nu$ progression significantly increases upon bias because the exciton becomes more localized as a result of the mixing with the heterojunction-confined S_1 state.

The low-lying S_{XT} also dominates the luminescence of HP and CP. The spectrum is composed mainly of the corresponding vibrational progression to the S_0 sublevels. The short-lived states above S_{XT} merely give rise to a small shoulder on the blue side of the zero-phonon feature, which appears most likely as a broadening in the actual emission. Thus we find that the theoretical rates for one-phonon and one-photon processes obtained within the present model generally agree with the fact that the electronic excitations in the real systems, no matter how created, relax to the bottom of the DOS prior to emission. A slight deviation from this rule is foreseen for the DP system. The zero-field emission spectrum shows a band above the optical gap that is due to the conversion-unstable but strongly optically coupled S_{XT} in this case. Still, the EL band shape of DP is foreseen to differ from that of HP and CP not because emission from the IC transients is stronger but because the main $S_1 \rightarrow S_0$ band is much weaker. As already pointed out, drive bias is expected to weaken the luminescence in HP and CP but to strengthen that of DP. The theoretical results suggest that, in the latter case, the $S_{XT} \rightarrow S_0$ band is so dominant that the delayed, red-shifted $S_1 \rightarrow S_0$ emission cannot be discerned in a steady-state experiment.

Finally, we note that although absorption and emission involve essentially one and the same excited electronic state S_{XT} spectral overlap is relatively small because of the Stokes shifts in the vibrational degrees of freedom. Emission and absorption differ in their electronic origins only for the DP system without bias, but with a theoretical luminescence lifetime of about 10 ns, the S_1 state is expected to enhance the nonradiative decay in that case.

IV. Conclusions

In an attempt to rationalize which molecular architecture would favor electroluminescence (EL) in organic semiconductors, we have simulated the recombination of an electron (e) and hole (h) in a single two-band homopolymer, a copolymer, and a diblock polymer. The process is resolved in terms of phonon-mediated interconversions within the excited density of states and radiative transitions to the ground state, with rates derived from a diabatic monoexcited configuration-interaction model. The results suggest that a copolymer with alternating acceptor and donor units A and D provides several advantages over the homopolymer with the same intraunit gap and interunit conjugation. First, the copolymer affords a lower barrier for the balanced $D^+...A^-$ charge injection. Second, the formation of an emissive exciton from the separated e−h pair is accelerated, reducing the probability for nonradiative decay. In this case, the DA polar structure destroys the e−h symmetry inherent to conjugated hydrocarbons and prevents the formation of long-lived charge-transfer intermediates. We anticipate that this result is relevant to the design of high-quantum-yield polymer materials, although the question of EL efficiency cannot be separated from those of singlet−triplet branching, interchain aggregation, and charge-carrier mobility.

A diblock polymer with an acceptor and a donor segment combines easy charge injection with current rectification. However, the electron and hole will tend to recombine nonradiatively at the block boundary by relaxing into a low-lying nonemissive defect state below the exciton. Thus, the model predicts a quantum yield from singlet e−h recombination that is about 4 times lower than that in a homopolymer or copolymer. The situation is foreseen to change significantly when drive bias is applied. For the homo- and copolymer, the quantum yield is found to decrease because preference is given to the formation of charge-transfer states that are not optically coupled to the ground state and consequently are likely to decay nonradiatively. In contrast, light emission from the diblock polymer is expected to increase and exceed that in periodic structures. This result is consistent with field-induced mixing between the block-boundary polar state and the exciton, resulting in an enhancement of the radiative recombination through both.

Acknowledgment. This work was supported by the National Science Foundation and by the Robert A. Welch Foundation.

References and Notes

(1) Chiang, C. K.; Fincher, C. R.; Park, Y. W.; Heeger, A. J.; Shirakawa, H.; Louis, E. J.; Gau, S. C.; MacDiarmid, A. G. *Phys. Rev. Lett*. **1977**, *39*, 1098.

(2) See for a review Friend, R. H.; Gymer, R. W.; Holmes, A. B.; Burroughes, J. H.; Marks, R. N.; Taliani, C.; Bradley, D. D. C.; Dos Santos, D. A.; Bredas, J. L.; Logdlund, M.; Salaneck, W. R. *Nature* **1999**, *397*, 121.

(3) McGehee, M. D.; Heeger, A. J. *Adv. Mater*. **2000**, *12*, 1655.

(4) McQuade, D. T.; Pullen, A. E.; Swager, T. M. *Chem. Rev.* **2000**, *100*, 2537.

(5) Sariciftci, N. S. *Curr. Opin. Solid State Mater. Sci.* **1999**, *4*, 373.

(6) Bao, Z. *Adv. Mater*. **2000**, *12*, 227. Sirringhaus, H.; Tessler, N.; Friend, R. H. *Science* **1998**, *280*, 1741.

(7) Heeger, A. J.; Kivelson, S.; Schrieffer, J. R.; Su, W. P. *Rev. Mod. Phys.* **1988**, *60*, 781.

(8) Hagler, T. W.; Packbaz, K.; Heeger, A. J. *Phys. Rev. B* **1994**, *49*, 10968.

(9) Lee, C. H.; Yu, G.; Moses, D.; Heeger, A. J. *Phys. Rev. B* **1994**, *49*, 2396.

(10) Rauscher, U.; Bässler, H.; Bradley, D. D. C.; Hennecke, M. *Phys. Rev. B* **1990**, *42*, 9830.

(11) Heun, S.; Mahrt, R. F.; Greiner, A.; Lemmer, U.; Bässler, H.; Halliday, D. A.; Bradley, D. D. C.; Burn, P. L.; Holmes, A. B. *J. Phys.: Condens. Matter* **1993**, *5*, 247.

(12) Bredas, J. L.; Cornil, J.; Heeger, A. J. *Adv. Mater*. **1996**, *8*, 447.

(13) Alvarado, S. F.; Seidler, P. F.; Lidzey, D. G.; Bradley, D. D. C. *Phys. Rev. Lett.* **1998**, *81*, 1082.

(14) Monkman, A. P.; Burrows, H. D.; Miguel, M. D.; Hamblett, I.; Navaratnam, S. *Chem. Phys. Lett.* **1999**, *307*, 303.

(15) Osterbacka, R.; Wohlgenannt, M.; Chinn, D.; Vardeny, Z. V. *Phys. Rev. B* **1999**, *60*, 11253.

(16) Wilson, J. S.; Dhoot, A. S.; Seeley, A. J. A. B.; Khan, M. S.; Köhler, A.; Friend, R. H. *Nature* **2001**, *413*, 828.

(17) Wohlgenannt, M.; Tandon, K.; Mazumdar, S.; Ramasesha, S.; Vardeny, Z. V. *Nature* **2001**, *409*, 494.

(18) Wohlgenannt, M.; Jiang, X. M.; Vardeny, Z. V.; Janssen, R. A. J. *Phys. Rev. Lett.* **2002**, *88*, 197401.

(19) Karabunarliev, S.; Bittner, E. R. *Phys. Rev. Lett*. **2003**, *90*, 057402.

(20) Cao, Y.; Parker, I. D.; Yu, G.; Zhang, C.; Heeger, A. J. *Nature* **1999**, *397*, 414.

(21) Kim, J. S.; Ho, P. K. H.; Greenham, N. C.; Friend, R. H. *J. Appl. Phys.* **2000**, *88*, 1073.

(22) Ho, P. K. H.; Kim, J. S.; Burroughes, J. H.; Becker, H.; Li, S. F. Y.; Brown, T. M.; Cacialli, F.; Friend, R. H. *Nature* **2000**, *404*, 481.

(23) Schweitzer, B.; Wegmann, G.; Hertel, D.; Mahrt, R. F.; Bässler, H.; Uckert, F.; Scherf, U.; Müllen, K. *Phys. Rev. B* **1999**, *59*, 4112.

(24) See for a review Joachim, C.; Gimzewski, J. K.; Aviram, A. *Nature* **2000**, *408*, 541.

(25) See for a review Metzger, R. M. *Acc. Chem. Res*. **1999**, *32*, 950.

(26) Aviram, A.; Ratner, M. A. *Chem. Phys. Lett.* **1974**, *29*, 277.

(27) Ng, M. K.; Yu, L. *Angew. Chem., Int. Ed*. **2002**, *42*, 3598.

(28) Ng, M. K.; Lee, D. C.; Yu, L. *J. Am. Chem. Soc.* **2002**, *124*, 11862.

(29) Karabunarliev, S.; Bittner, E. R. *J. Chem. Phys*. **2003**, *118*, 4291.

(30) Karabunarliev, S.; Bittner, E. R. *J. Chem. Phys.* **2003**, *119*, 3988.

(31) Pariser, R.; Parr, R. G. *J. Chem. Phys*. **1953**, *21*, 767. Pople, J. A. *Trans. Faraday Soc*. **1953**, *42*, 1375.

(32) Holstein, T. *Ann. Phys.* **1959**, *8*, 325.

(33) Karadakov, P.; Calais, J. L.; Delhalle, J. *J. Chem. Phys*. **1991**, *94*, 8520.

(34) Mataga, N.; Nishimoto, K. *Z. Phys. Chem*. **1957**, *13*, 140.

(35) Pichler, K.; Halliday, D. A.; Bradley, D. D. C.; Burn, P. L.; Friend, R. H.; Holmes, A. B. *J. Phys.: Condens. Matter* **1993**, *5*, 7155.

(36) Cornil, J.; Beljonne, D.; Heller, C. M.; Campbell, I. H.; Laurich, B. K.; Smith, D. L.; Bradley, D. D. C.; Müllen, K.; Bredas, J. L. *Chem. Phys. Lett.* **1997**, *278*, 139.

(37) Lim, S. H.; Bjorklund, T. G.; Bardeen, C. J. *Chem. Phys. Lett*. **2001**, *342*, 555.
(38) Beljonne, D.; Shuai, Z.; Pourtois, G.; Bredas, J. L. *J. Phys. Chem. A* **2001**, *105*, 3899.
(39) Burin, A. L.; Ratner, M. A. *J. Chem. Phys*. **1998**, *109*, 6092.
(40) Kasha, M. *Discuss. Faraday Soc*. **1950**, *9*, 14.
(41) Harrison, N. T.; Hayes, G. R.; Phillips, R. T.; Friend, R. H. *Phys. Rev. Lett.* **1996**, *77*, 1881.
(42) Samuel, D. W.; Rumbles, G.; Friend, R. H. In *Primary Excitations in Conjugated Polymers: Molecular Exciton versus Semiconductor Band Model*; Sariciftci, N. S., Ed.; World Scientific: Singapore, 1997; p 140.
(43) May, V.; Kühn, O. *Charge and Energy Transfer Dynamics in Molecular Systems*; Wiley-VCH: Berlin, 2000.
(44) Mukhopadhyay, D.; Hayden, G. W.; Soos, Z. G. *Phys. Rev. B* **1995,** *51*, 9476.
(45) Yu, Z. G.; Saxena, A.; Bishop, A. R. *Phys. Rev. B* **1997**, *56*, 3697.
(46) Chandross, M.; Mazumdar, S. *Phys. Rev. B* **1997**, *55*, 1497.
(47) Stevens, M. A.; Silva, C.; Russell, D. M.; Friend, R. H. *Phys. Rev. B* **2000**, *63*, 165213.
(48) Cornil, J.; Gueli, I.; Dkhissi, A.; Sancho-Garcia, J. C.; Hennebicq, E.; Calbert, J. P.; Lemaur, V.; Beljonne, D.; Bredas, J. L. *J. Chem. Phys.* **2003**, *118*, 6615.
(49) Blom, P. W. M.; Dejong, M. J. M.; Breedijk, S. *Appl. Phys. Lett.* **1997**, *71*, 930.
(50) Arias, A. C.; MacKenzie, J. D.; Stevenson, R.; Halls, J. J. M.; Inbasekaran, M.; Woo, E. P.; Richards, D.; Friend, R. H. *Macromolecules* **2001**, *34*, 6005.
(51) Morteani, A. C.; Dhoot, A. S.; Kim, J.; Silva, C.; Greenham, N. C.; Murphy, C.; Moons, E.; Cina, S.; Burroughes, J. H.; Friend, R. H. *Adv. Mater*. **2003**, *15*, 1708.
(52) Morteani, A. C.; Sreearunothai, P.; Herz, L. M.; Friend, R. H.; Silva, C.; *Phys. Rev. Lett.*, submitted for publication, 2003.
(53) Mao, G.; Fischer, J. E.; Karasz, F. E.; Winokur, M. J. *J. Chem. Phys*. **1993**, *98*, 712.
(54) Johnston, M. B.; Herz, L. M.; Khan, A. L. T.; Köhler, A.; Davies, A. G.; Linfield, E. H. *Chem. Phys. Lett.* **2003**, *377*, 256.
(55) Karabunarliev, S.; Bittner, E. R.; Baumgarten, M. *J. Chem. Phys*. **2001**, *114*, 5863.